buildings

IMPACT FACTOR 3.8

CITESCORE 3.1

Article

Multi-Zone Infection Risk Assessment Model of Airborne Virus Transmission on a Cruise Ship Using CONTAM

Zhuang Xia, Hang Guan, Zixuan Qi and Peng Xu

MDPI

https://doi.org/10.3390/buildings13092350

buildings

MDPI

Article

Multi-Zone Infection Risk Assessment Model of Airborne Virus Transmission on a Cruise Ship Using CONTAM

Zhuang Xia, Hang Guan, Zixuan Qi and Peng Xu *

School of Mechanical Engineering, Tongji University, Shanghai 200092, China; 2130277@tongji.edu.cn (Z.X.); guanhang1998@163.com (H.G.); alexkey@tongji.edu.cn (Z.Q.)
* Correspondence: xupeng@tongji.edu.cn

Abstract: Since the onset of the pandemic, the cruise industry has faced substantial challenges, experiencing an 81% year-on-year decline in 2020. Notably, China's cruise industry has remained shuttered for nearly two years. The conventional epidemiological investigations relying on human memory have proven inadequate in regard to swiftly and reliably identifying high-risk populations, thus leading to excessive pandemic prevention or other inappropriate measures. Furthermore, current research endeavors have not adequately addressed the critical issues of isolation location selection and the estimation of isolation scale within multi-zone indoor environments. Therefore, how to control the epidemic with minimal impact on the public has become an urgent problem. To solve the problems mentioned above, a multi-zone infection risk assessment model of airborne virus transmission was proposed to rapidly qualify the risk of infection, identify the high-risk population, and provide guidance. The model can be divided into two parts, including a multi-zone airflow model and a risk assessment model based on the Wells–Riley model. A large in-service ro-ro passenger ship already in service was used for the application of the proposed method. The results show that the number of isolated rooms shall be at least 5% of the occupancy and the isolation location can be chosen through the multi-zone infection risk assessment model. This paper provides insights into risk assessment to mitigate the spread of epidemics on a large cruise ship, and the method can be easily applied to all kinds of multi-zone indoor environments.

Keywords: multi-zone airflow simulation; virus airborne transmission; risk assessment model; large cruise ship

Citation: Xia, Z.; Guan, H.; Qi, Z.; Xu, P. Multi-Zone Infection Risk Assessment Model of Airborne Virus Transmission on a Cruise Ship Using CONTAM. *Buildings* **2023**, *13*, 2350. https://doi.org/10.3390/buildings13092350

Academic Editor: Cinzia Buratti

Received: 2 August 2023
Revised: 7 September 2023
Accepted: 13 September 2023
Published: 15 September 2023

1. Introduction

Since the outbreak caused by SARS-CoV-2 in December 2019, clustered transmission of SARS-CoV-2 on cruise ships has occurred in many locations worldwide [1]. Owing to the characteristics of high cabin airtightness, weak natural ventilation, high population density, crowded public and living spaces, and shared public health facilities and supplies, community transmission is prone to occur within a cruise ship once a case of SARS-CoV-2 infection occurs. One study found that countries with arrival and departure ports and ports that continued to accept cruise ships until March 2020 had higher rates of SARS-CoV-2 infection than those without such ports [2]. The second round of epidemic transmission in China seems to have begun since early May 2023. The COVID-19 outbreak has posed severe challenges to the cruise industry. To reduce the transmission, the World Health Organization, State Departments, European Center for Disease Control and Prevention (ECDC), American Society of Heating, Refrigerating and Air-Conditioning Engineers (ASHRAE), and Chinese Society of Refrigeration have issued guidelines for epidemic control [3]. The role of the HVAC system in the spread of the virus has been considered. According to these guidelines, strengthening ventilation is the main engineering control measure, and it can be supplemented with high-efficiency filters, operation strategies for air-conditioning systems, and other epidemic prevention and control measures. However,

these recommendations are crude and lack the effective suggestions for the estimation of the isolation scale.

Research methods for virus transmission and infection risk assessments can be divided into three categories [4]: mathematical models (such as the Wells–Riley model, optimized Wells–Riley model, other exponential dose–response models, and the β-Poisson distribution model), computational fluid dynamics (CFD), and integrations of mathematical models and numerical simulations.

The most used mathematical model for estimating airborne transmission risk is the Wells–Riley model proposed by Riley in 1978 [5]; it is based on the concept of quantum infection. The typical Wells–Riley model assumes that the air in the space is well mixed at a steady state, the elimination of infectious particles caused by filtration and deposition is ignored, and any biological decay of the virus is not considered. This model has been widely used to assess the airborne risk of many respiratory diseases [6,7], including influenza, tuberculosis, severe acute respiratory syndrome (SARS-CoV-1), Middle East respiratory syndrome (MERS), and measles. Subsequently, the Wells–Riley model was improved by other researchers. Rudnick and Milton [8] proposed the concept of fractional rebreathing in 2003 and used it to modify the Wells–Riley model under transient conditions; however, the optimized Wells–Riley model is also based on the assumption of good mixing. Other researchers have extended the Wells–Riley model to include unstable exposure [9] and incomplete mixing [10]. Zhang et al. [9] proposed a dilution-based method for assessing the risk of airborne infection, and this model is a comprehensive extension of the Wells–Riley model with spatial and temporal resolution. Aganovic et al. [11] studied the impact of different indoor relative humidity values on the risk of SARS-CoV-2 transmission based on the improved Wells–Riley model, and the results show that controlling indoor humidity at 40–60% is not an effective means of reducing the risk of new crowd infections, while strengthening ventilation is a more effect strategy. Ville Vuorinen et al. [12] introduced a dynamic source term in the Wells–Riley model equation to simulate the spatiotemporal dependence of aerosols, and the risk of virus infection in supermarkets and bars was evaluated and compared with the results of the typical Wells–Riley model.

CFD simulations employ software tools such as ANSYS to model and analyze the distribution of SARS-CoV-2 in specific scenarios, enabling a comprehensive assessment of transmission risk. Borro et al. [13] used CFD to simulate the spread of SARS-CoV-2 in waiting rooms and wards under different air volumes of HVAC systems and evaluated the role of HVAC systems in the virus transmission process. Yamakawa et al. [14] simulated the long-term (90 min) spread of virus droplets in the classroom when a teacher was infected with COVID-19, and a safe distance between students and the teacher was proposed. However, this type of research can only provide the relative risk of exposure based on the relative size of the viral aerosol concentration and cannot provide the probability of infection at a specific viral aerosol concentration.

A combination of mathematical modeling and CFD simulation was also adopted in which the Wells–Riley model was integrated with CFD to quantify the risk of viral infection [15]. Wang et al. [4] integrated CFD simulations and Wells–Riley models to quantify the probability of COVID-19 infection among passengers traveling long distances by train. Yan et al. [16] simulated the transmission characteristics of aerosols generated by a cough in a Boeing 737 cabin. The results were integrated into the Wells–Riley equation to estimate the infection risk. The infection probabilities estimated by the Wells–Riley model and CFD were compared in a typical classroom scenario, with or without mechanical ventilation. In the scenario without mechanical ventilation, the results were consistent, whereas in the scenario with mechanical ventilation, an error of 29% was observed [17].

Several studies have been conducted on the transmission risk of SARS-CoV-2 on cruise ships, based on theoretical analysis. Pang et al. [18] constructed a risk assessment framework based on the possibility and dangers of the spread of SARS-CoV-2 in a closed marine environment. Zhang et al. [1] established a Bayesian network model of the infection risk of COVID-19 for large cruise passengers based on data collected on confirmed cases,

and the seventh edition of the "COVID-19 Diagnosis and Treatment Program" issued by the National Health Commission. The model was validated using historical data.

At present, airflow simulations for epidemic risk assessment are mostly aimed at a single zone within a building [13,14] and do not consider the air flows between zones (air circulation caused by the movement of people, the opening and closing status of doors and windows, and the form and operation strategy of the air-conditioning system). The multi-zone airflow model assumes that air is well mixed in a zone, unable to check local airflow conditions [19]. Different from the multi-zone model, computational fluid dynamics (CFD) decomposes a building zone into a large amount of control volumes and can provide detailed description of the airflow by solving the Navier–Stokes equations [20].

Generally, the multi-zone airflow simulation is mainly used for ventilation and pollutant diffusion analysis. Wang et al. [21] studied the effect of heating by charcoal basin in a rural residence in Hunan Province on the indoor air quality in winter, using the multi-zone airflow model. A multi-zone airflow model was established through CFD simulations to study the airflow rate and aerosol concentration with wind pressure impact in a certain apartment floor and corridor [22]. Szczepanik-Scislo [23] studied how an air terminal device influenced the air quality through multi-zone and CFD simulation, where multi-zone simulation was conducted in CONTAM. Heibati et.al [24] developed an integrated model that combined CONTAM and WUFI (a software for state-of-the-art hygrothermic analysis) to assess the indoor air quality.

Multi-zone airflow simulations are rarely used for epidemic risk assessments on cruise ships; they are mostly used on buildings. In 2021, Pease et al. [25] evaluated the concentrations and probabilities of infection for both building interior and exterior exposure sources using a well-mixed model in a multiroom building served by a central air-handling system. In 2022, Yan et al. [26] evaluated several engineering mitigation strategies for five selected US Department of Energy prototype commercial buildings by using a combined multi-zone airflow model and Wells–Riley model.

Obviously, the conclusions driven from single-zone airflow simulations cannot be directly applied for epidemic control or risk assessments of a multi-zone indoor environment. Owing to the characteristics of high cabin airtightness, weak natural ventilation, high population density, and shared public health facilities, virus transmission may be different from that in buildings. Therefore, the development of a risk assessment model based on the holistic layout of the cruise ships to target the risk groups quickly and reliably and estimate the isolation scale is of great significance. This study attempts to fill in this knowledge gap. This paper establishes a multi-zone infection risk assessment model to guide the formulation of prevention and control strategies for cruise ships during the epidemic (including the identification of high-risk groups, strategic placement of isolation points, and determination of isolation scale and operation management of air-conditioning systems) and provides a reference for cruise designers to divide the functional areas of a cruise ship and design air-conditioning systems. This is the first time that a multi-zone airflow model combined with the Wells–Riley model was applied for ships.

Based on the existing literature, we identify the following challenging questions:

When COVID-19 patients appear in a cruise ship, how do we quantify the risk of virus infection in different rooms to guide decision making?

How do we choose a temporary isolation area in a multi-zone environment when patients cannot be transferred out?

Are there any efficient measures to control virus transmission in an emergency and evaluate the effectiveness of several epidemic prevention and control measures?

2. Methodology

The proposed method mainly contains two steps, as shown in Figure 1. In step one, a multi-zone airflow model corresponding to the real model was established using CONTAM 3.4, a software program developed by National Institute of Standards and Technology (NIST) to simulate the virus spread process: (1) Simplify the object into a set of zones that

are relevant to your goal in performing an analysis. (2) Draw a specific cruise ship model. (3) Establish an HAVC system for the ship. (4) Collect and input data associated with each of the model components, including air leakage paths (windows, doors, and cracks), ventilation system elements, and contaminant sources. The virus concentration of each area was output from CONTAM after simulation. In step two, a risk assessment model was established using the Wells–Riley model to calculate the infection possibility. Finally, we evaluated the effect of adding area partitions and adding filters on the spread of the virus.

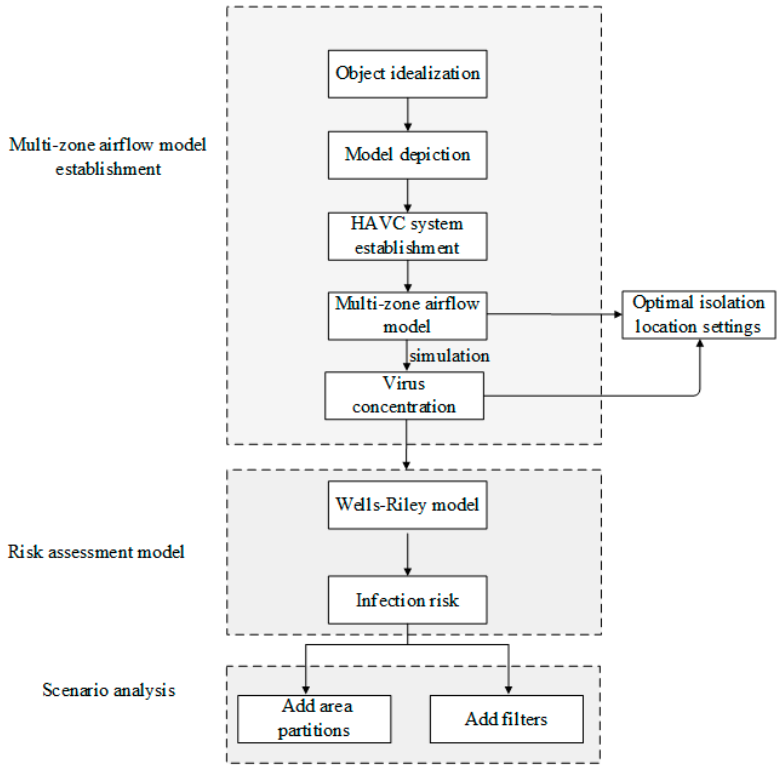

Figure 1. The framework of the proposed method.

2.1. Multi-Zone Airflow Model

CONTAM, which is a computer program for multi-zone indoor air quality and ventilation analysis, was used to construct the multi-zone airflow model. CONTAM can calculate infiltration and exfiltration airflows between interior zones of the building and the outdoors, room-to-room airflows, and ventilation system airflows. These airflows are the result of pressure differences resulting from driving forces, which include mechanical ventilation system fans, wind pressures acting on the exterior of the building, and buoyancy effects induced by temperature differences between zones, including the outdoors [27].

A multi-zone airflow model consists of zones, airflow paths, and an air-conditioning system, as shown in Figure 2. Rooms are segregated into distinct zones based on their physical boundaries. There is air supply and air return through the air-conditioning system in each zone. By establishing the airflow network model corresponding to the research object, the airflow pattern, as well as the physical parameters of each area (including pressure, and pollutant concentration), under different HVAC operating modes can be calculated.

The multi-zone airflow model in our study is based on the following simplification. Firstly, simulations in CONTAM are based on the assumption of instantaneously well-mixed zones. Secondly, the airflow paths used primarily encompass doors and cracks between doors and its frame, with no consideration given to air infiltration through closed windows. Finally, the diffusion of pollutants through the HVAC system is not considered. We assume that the air supply through the air-conditioning system is clean.

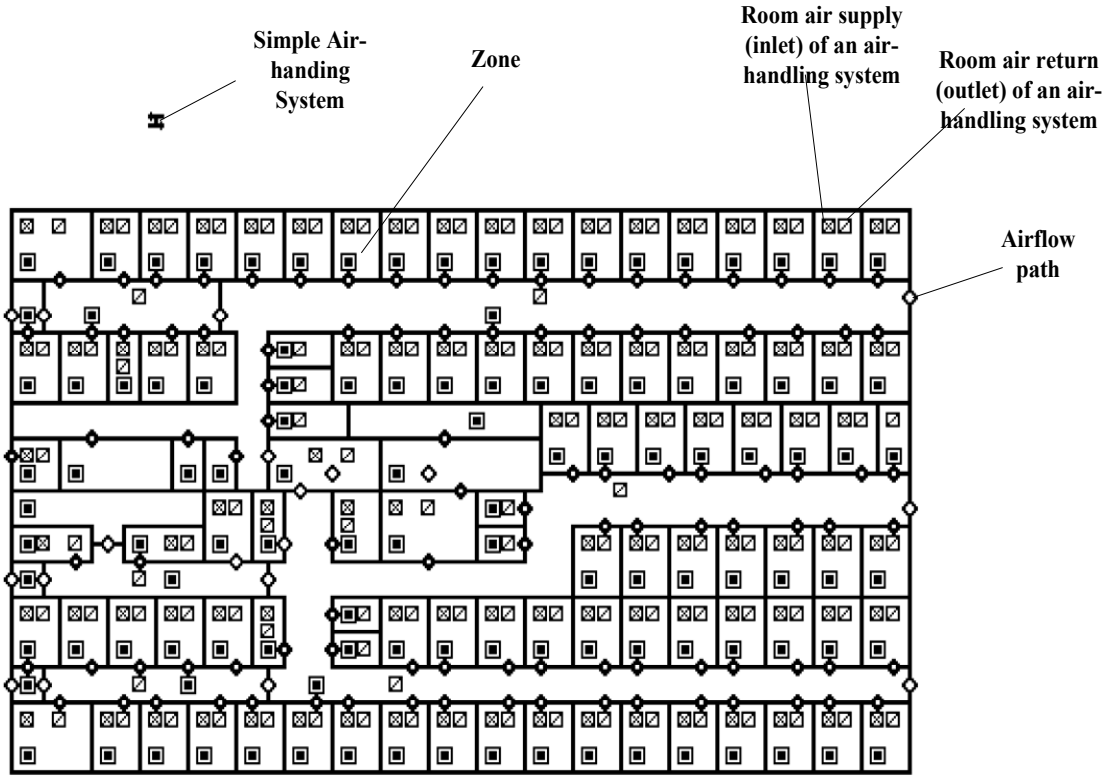

Figure 2. Airflow model constructed in CONTAM for C area in 9th floor (C area in 9th floor refers to the right third of the 9th floor of the ship).

Before establishing the multi-zone airflow model, cruise ship information needs to be collected, as shown in Table 1.

Table 1. Detailed information about cruise ship.

Category	Information	Data Source	Associated CONTAM Object
Geometry	Room volume	Calculation manual + architectural drawings	Zone
	Room floor area	Calculation manual + architectural drawings	Zone
	Cruise layout	Architectural drawings	Zone
HVAC system	Room temperature	Calculation manual	Zone
	Supply air volume of the rooms	Calculation manual + architectural drawings	Air-handling system
	Return air volume of the rooms	Calculation manual + architectural drawings	Air-handling system
	Airflow path	Architectural drawings	Airflow path
Virus	Generation rate	The literature	Contaminant
	Mean diameter	The literature	Contaminant
	Diffusion coefficient	The literature	Contaminant

2.2. Risk Assessment Model

We adopted the Wells–Riley model to describe the relationship between the air exchange rate and infection probability and then established a risk assessment model. A specific model was built using Python 3.10.

The Wells–Riley model is a classical model for estimating the steady-state infection risk via airborne transmission in a well-mixed space [3]:

Wells–Riley model:

$$P_I = \frac{C}{S} = 1 - e^{-\frac{Iqpt}{Q}} \quad (1)$$

where P_I is the infection possibility; C is the new infection cases; S is the susceptible cases; I is the number of infectors; p is the inhalation rate, m^3/h; q is the emission rate of infectious quanta per infector, quantum/h; one quantum in the model represents an infectious dose that would infect 63% of the population with the exposure per the Wells–Riley model [3]; and t is the exposure time, h.

In our study, the virus concentration inside the room was simulated using a multi-zone airflow model. Therefore, the probability of infection for one person per room is calculated as shown in Function (2):

$$P_I = 1 - e^{-atm \times p \times t} \quad (2)$$

where P_I is the infection possibility; atm is the contaminant concentration (quantum/m^3); p is the inhalation rate (m^3/h), and it is set as 0.36 m^3/h [14]; and t is the exposure time (h), and it is set as 1. In our model, t is a flexible variable that can be changed according to the preference of the researchers.

2.3. Infection Risk Assessment Index

Under certain circumstances, this study used the number of virus spread areas and the estimated number of infected people in the entire ship to quantitatively evaluate the infection risk.

The infection risk of the whole ship was estimated by the following formula:

$$n = \sum P_i \times n_i \quad (3)$$

where n is the estimated number of people infected in the entire ship, P_i is the infection possibility for each zone, and n_i is the person indoors for each zone. The calculation of n is based on a hypothesis: each area where the virus exists has a 50% occupancy, which was estimated by staff on the ship in case study.

3. Case Study

A large in-service ro-ro passenger ship was simulated in CONTAM, as shown in Figure 3. The ship has ten floors in total. The floors below floor 7 are used for freight transportation, and the personnel activity areas are on floors 7, 8, and 9, containing restaurant, galley, cabins, office, and so on. Each floor has three main areas, i.e., A, B, and C. The layout is shown in Appendix A. There are 175 passenger cabins and 46 crew cabins. The passenger capacity of the ship is above 350. The HVAC system on this ship is constant air volume central air-conditioning system. Systems of 100% fresh air are supplied with energy recovery by enthalpy exchangers, but that the wheelhouse is provided with a dedicated air-conditioning system of 35% fresh air. Moreover, the temperature and relative humidity in the air-conditioned area on board are set to 24 °C and 60%.

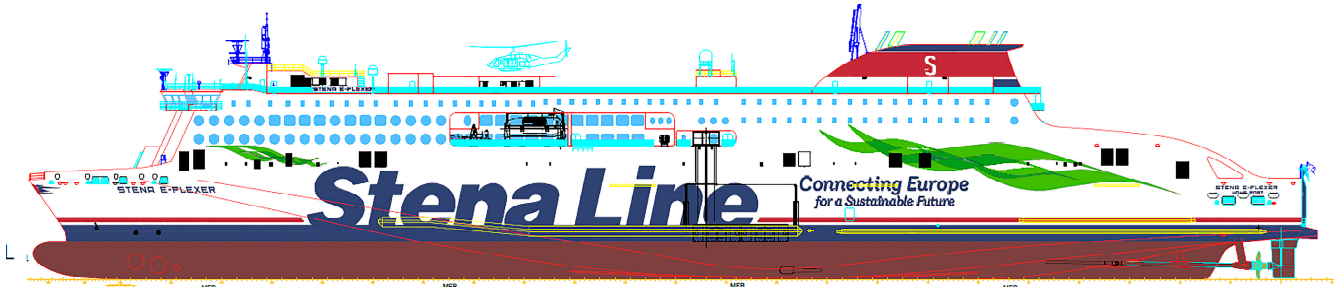

Figure 3. Appearance of the ship.

The airflow model corresponding to the ship layout was constructed in CONTAM.

Adrian Esterman, a former WHO epidemiologist, believes that the infection rate of Omicron BA.2 is equivalent to that of measles. The Basic Reproduction Number (R0) for Omicron BA.2 has surged to 12, which is six times that of the original virus [28]. Omicron BA.2 has thus emerged as an exceptionally contagious pathogen, akin to measles, which typically exhibits an R0 range of 12–18 [29], and the R0 of BA.5 has reached 18.6 [27]. Indeed, R0, or the Basic Reproduction Number, serves as a measure of a pathogen's transmission potential, with higher values signifying a greater capacity for dissemination. Therefore, we opted to model our scenarios based on measles in our simulations. The relevant parameters of measles were set as shown in Table 2.

Table 2. Setting of the parameter for measles in CONTAM.

Species Properties	Setting
Molar mass	20 kg/kmol
Diffusion coefficient	2×10^{-5} m^3/s
Mean diameter	5×10^{-6} mm
Effective density	1 kg/m^3
Specific heat	100 J/(kg·K)

According to Riley et al. [3], the quantum of measles is between 570/h and 5600/h, and the commonly used value in previous studies is 5480/h. In this case, the quantum of the measles virus was set to 5480/h for the simulation.

3.1. Optimal Isolation Location Settings

An isolation room refers to a cabin for people confirmed or suspected of having an infection on board, and it is equipped with independent or designated dedicated toilets. To ensure that the isolation room had an independent toilet and was far away from the public area, an isolation area was placed in a cabin area. For this ship, the isolation area should be set in the area C on the eighth or ninth floor. Next, the area C on the ninth floor was taken as an example to illustrate the selection steps and basis. Although the optimal isolation locations are different for various ships, the method for determining the isolation locations in this study is universal.

3.1.1. Room Category Division

First, corridors with walls and doors were set as boundaries and divided into five areas, which were numbered 9C-97, 9C-98, 9C-99, 9C-100, and 9C-102, as illustrated in Figure 4.

The rooms were then divided into three categories according to the number of rooms adjacent to the corresponding corridor; that is, the number of rooms adjacent to the corresponding corridor determined the category of these rooms. Thus, when a virus is detected in a corridor, a greater number of rooms in contact with the corridor correspond to a greater number of rooms at risk of infection.

In our simulation, corridors 9C-97, 9C-102, and 9C-99 and their adjacent rooms are first-class areas; corridor 9C-98 and its adjacent rooms are second-class areas; and corridor 9C-100 and its adjacent rooms are third-class areas. The results are shown in Table 3.

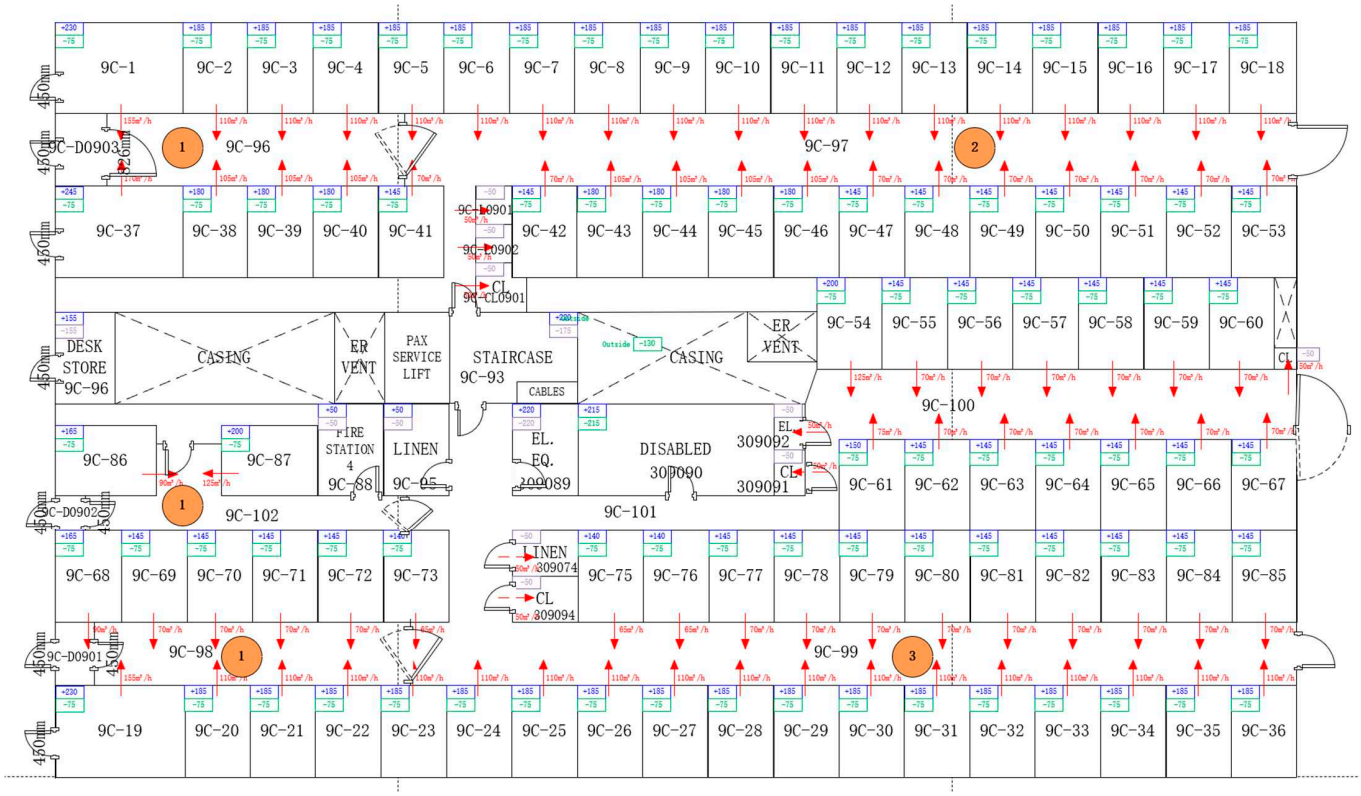

Figure 4. Corridor division results.

Table 3. Corridor and adjoining room division results.

Corridor Number	Adjoining Rooms	Number of Adjoining Rooms	Room Category
9C-97	9C-1~9C-5, 9C-37~9C-41	10	1
9C-98	9C-6~9C-18, 9C-42~9C-53	25	2
9C-99	9C-68~9C-73, 9C-19~9C-23	10	1
9C-100	9C-54~9C-67, 9C-75~9C-85, 9C-24~9C-36, 9C-90	38	3
9C-102	9C-86~9C-88	3	1

3.1.2. Typical Room Infection Risk Analysis

A typical room was selected from each of the three categories of areas in the above subsection for the scenario analysis.

(1) **Scenario analysis for rooms belonging to the first category**

Room 9C-1 was selected as a typical room for the first category. The infection risk of each room in the ship is shown in Table 4 for when an infected person stays in 9C-1.

Table 4. Infection risk of each room when an infected person is in C9-1.

Infected Person is in 9C-1				
Floor	**Room**	**After 1 h (Quanta/m^3)**	**After 4 h (Quanta/m3)**	**Risk_P**
<9>	9C-1	23.834	23.908	1.000
<9>	9C-97	1.035	1.038	0.312
<9>	9C-D0903	0.967	0.970	0.295

Note: The third column of the table labeled 3600 indicates the virus concentration in the zone after the patient has stayed for an hour, and the fourth column indicates 4 h. The infection risk (i.e., risk_P) was calculated based on the stable virus concentration.

(2) **Scenario analysis for rooms belonging to the second category**

Room 9C-9 was selected as a typical room for the second category. The infection risk of each room in the ship is shown in Table 5 for when an infected person is located in 9C-9.

Table 5. Infection risk of each room when an infected person is in 9C-9.

Infected Person is in 9C-9				
Floor	**Room**	**After 1 h (Quanta/m^3)**	**After 4 h (Quanta/m^3)**	**Risk_P**
<9>	9C-9	29.717	29.723	1.000
<9>	9C-L0901	0.639	0.640	0.206
<9>	9C-98	0.640	0.640	0.206
<9>	9C-CL0901	0.639	0.640	0.206
<9>	9C-L0902	0.639	0.640	0.206
<9>	9C-97	0.484	0.484	0.160
<9>	9C-D0903	0.452	0.452	0.150

(3) **Scenario analysis for rooms belonging to the third category**

Room 9C-36 was selected as the typical room for the third category. The infection risk of each room in the ship is shown in Table 6 for when an infected person is located in 9C-36.

Table 6. Infection risk of each room when an infected person is in C9-36.

Infected Person Is LOCATED in9C-36				
Floor	**Room**	**After 1 h (Quanta/m^3)**	**After 4 h (Quanta/m^3)**	**Risk_P**
<9>	9C-36	29.717	29.723	1.000
<9>	9C-CL0902	0.387	0.387	0.130
<9>	9C-91	0.387	0.387	0.130
<9>	9C-100	0.387	0.387	0.130
<9>	9C-94	0.378	0.387	0.130
<9>	9C-92	0.386	0.387	0.130
<9>	9C-74	0.378	0.387	0.130
<9>	9C-D0902	0.356	0.357	0.120
<9>	9C-102	0.356	0.357	0.120
<9>	9C-99	0.289	0.290	0.099
<9>	9C-D0901	0.279	0.279	0.096

From the results of the infection risk of typical rooms in the above three types of areas, when a patient is in the rooms belonging to the first category, the impact on other rooms is small, and only three zones are affected. However, when a patient is in the rooms belonging to the third category, 11 zones are affected. The affected area range was relatively large. Therefore, rooms belonging to the first category are more suitable as isolation areas according to the above analysis results.

3.2. Infection Risk Evaluation in Public Areas

If a patient previously visited a public area and the number of people and rooms involved was relatively large, then the staff should promptly disinfect the involved locations and investigate the personnel who have visited the location. Moreover, the locations that should be treated as the initial key areas when many locations are involved in this scenario must be identified. Therefore, the risk of infection in other rooms must be determined when a case occurs in a public area. Therefore, we can select the key locations for disinfection and check the personnel who have visited these locations.

When a patient visits a public area, the virus spreads widely. To provide guidance for various emergency measures (such as specific isolation areas, materials, caregivers, etc.), estimating the total number of infected individuals based on the calculated infection risk and normal number of people in each zone is necessary.

We simulated the scenario of a patient located in several typical zones and calculated the estimated total number of infected patients, as shown in Figure 5.

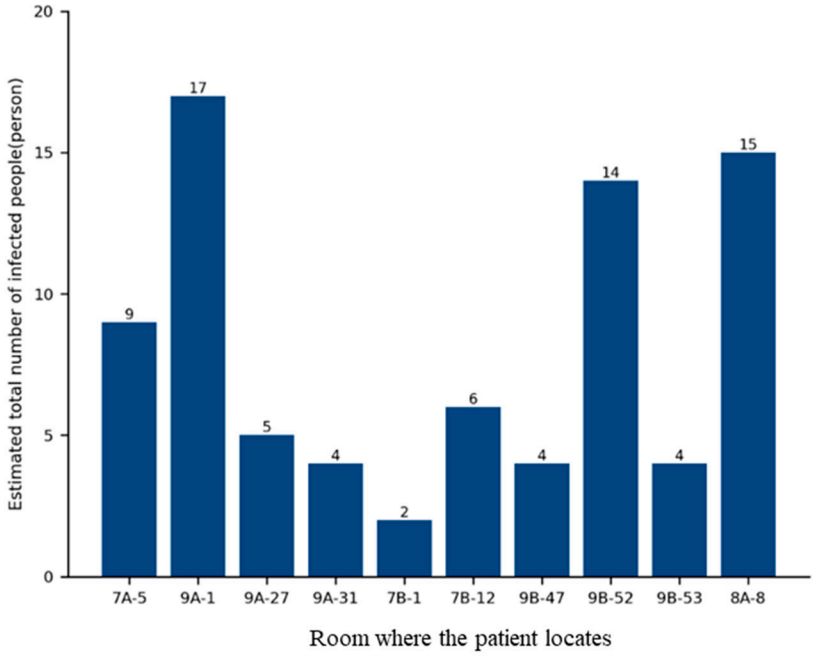

Figure 5. Histogram of the estimated total number of infected people when the patient visited a typical public area.

According to the calculation results, in the most proliferative scenario, that is, when the patient is in 9C-1, the maximum number of infected patients is estimated at 17. The number of isolation rooms in the first round of diffusion can be determined according to the scale of the number of infected individuals; that is, approximately 17 independent cabins are needed for isolation. Because we consider only the first round of epidemic transmission, it is recommended that the number of isolated rooms shall be at least 5% of the occupancy.

3.3. Building Layout and System Optimization

3.3.1. Adding Area Partitions

To study the effect of adding area partitions on the spread of the virus, it was assumed that the patient was in cabin 9C-18 and the long corridor in area C on the ninth floor was physically partitioned by doors. This study analyzed the impact of virus spread under five scenarios: no increase in partitions, add three partitions every six rooms, add two partitions every eight rooms, add one partition every ten rooms, and add one partition every twelve rooms. Figure 6 shows the layout of the ship in the five cases, and the yellow sections in the figure represent the positions of the partition.

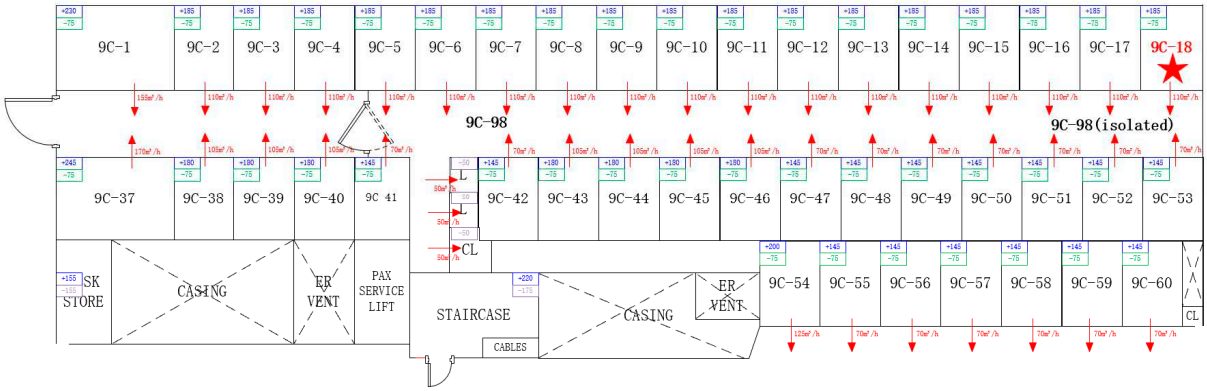

(**a**) No increase in partitions.

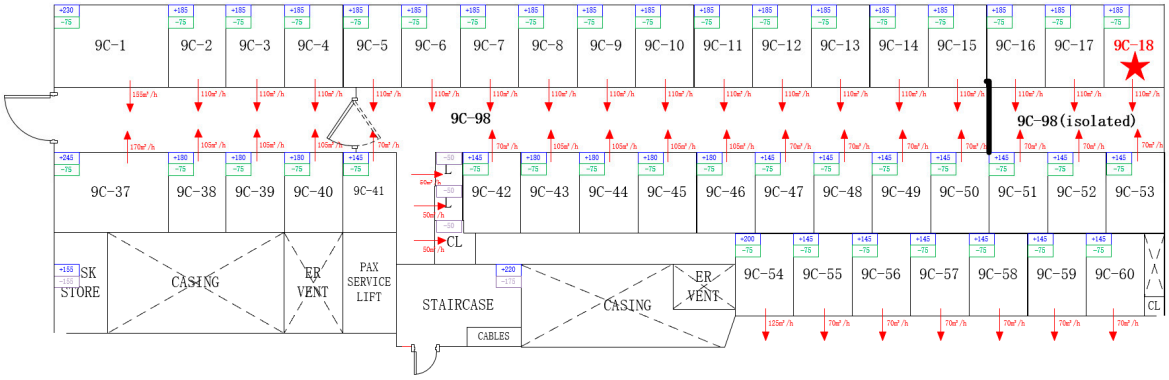

(**b**) Add three partitions every 6 rooms.

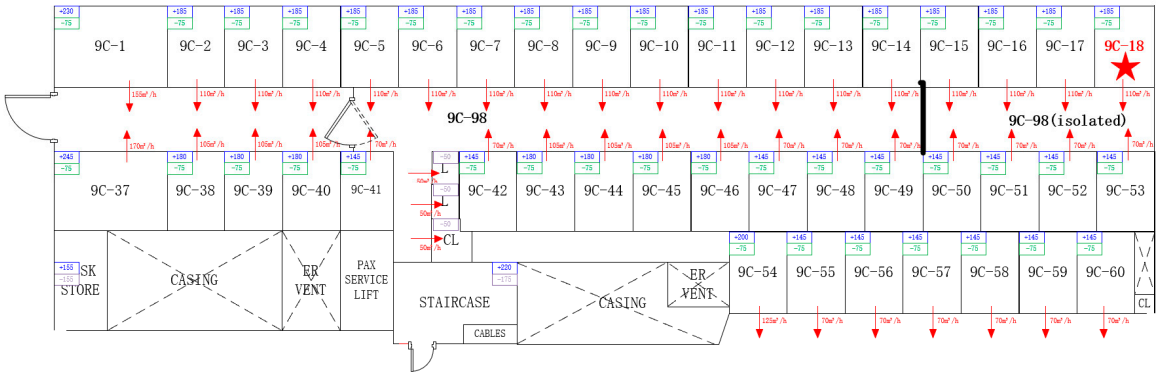

(**c**) Add two partitions every 8 rooms.

Figure 6. *Cont.*

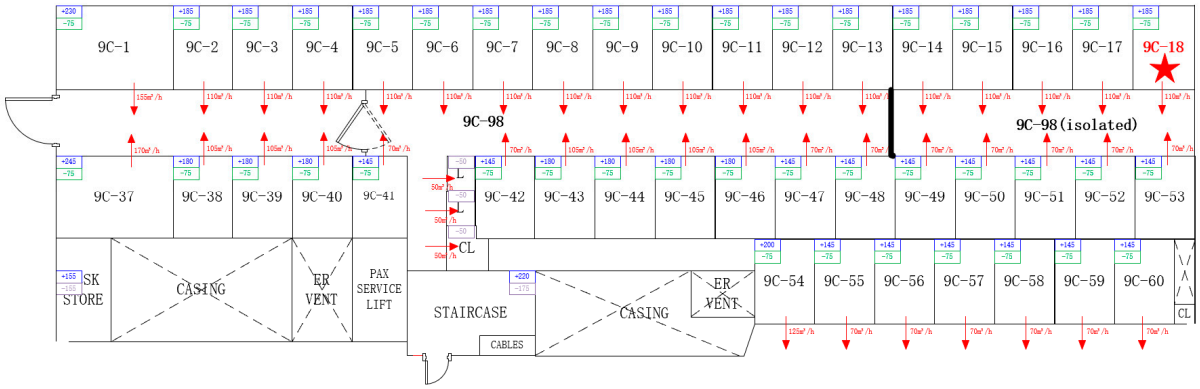

(**d**) Add one partition every 10 rooms.

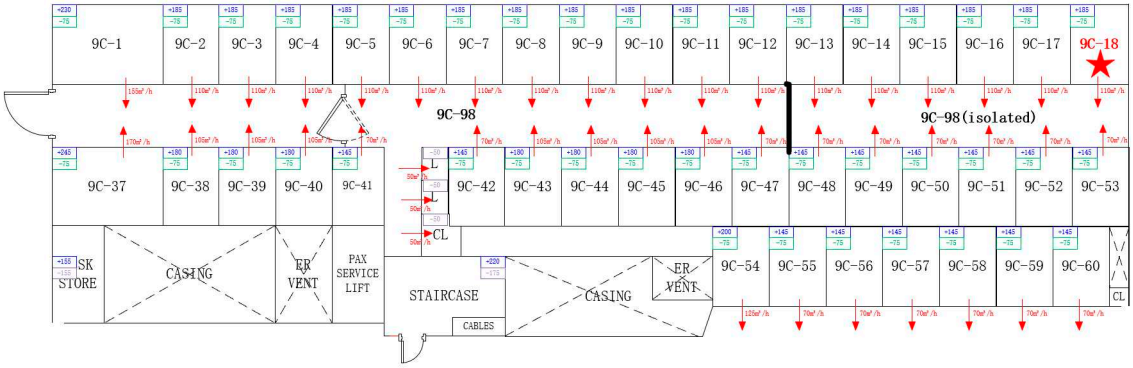

(**e**) Add one partition every 12 rooms.

Figure 6. The corridor under five scenarios. (The position of the red five-pointed star is the position of the patient, and the black thick solid line is the position of the increased partitions).

When the patient was in cabin 9C-18, doors were added to corridor C9-98 to create a physical partition. The spread of the virus in each zone before and after partitioning is shown in Table 7 and Figure 7.

Table 7. Virus stable concentration and infection risk before and after adding a partition (x_virus means the virus stable concentration of adding one partition every x room, quanta/m3; x_risk means infection probability).

Zone	0_virus	0_risk	6_virus	6_risk	8_virus	8_risk	10_virus	10_risk	12_virus	12_risk
9C-18	29.723	1.000	29.723	1.000	29.723	1.000	29.723	1.000	29.723	1.000
9C-CL0901	0.640	0.206	0.577	0.188	0.448	0.149	0.542	0.177	0.546	0.178
9C-L0901	0.640	0.206	0.577	0.188	0.448	0.149	0.542	0.177	0.546	0.178
9C-L0902	0.640	0.206	0.577	0.188	0.448	0.149	0.542	0.177	0.546	0.178
9C-97	0.484	0.160	0.434	0.145	0.335	0.113	0.407	0.136	0.410	0.137
9C-D0903	0.452	0.150	0.404	0.136	0.312	0.106	0.380	0.128	0.382	0.129
9C-98	0.640	0.206	0.577	0.188	0.448	0.149	0.542	0.177	0.546	0.178
9C-98 (isolated by partition)			1.645	0.447	1.707	0.459	1.406	0.397	1.330	0.381

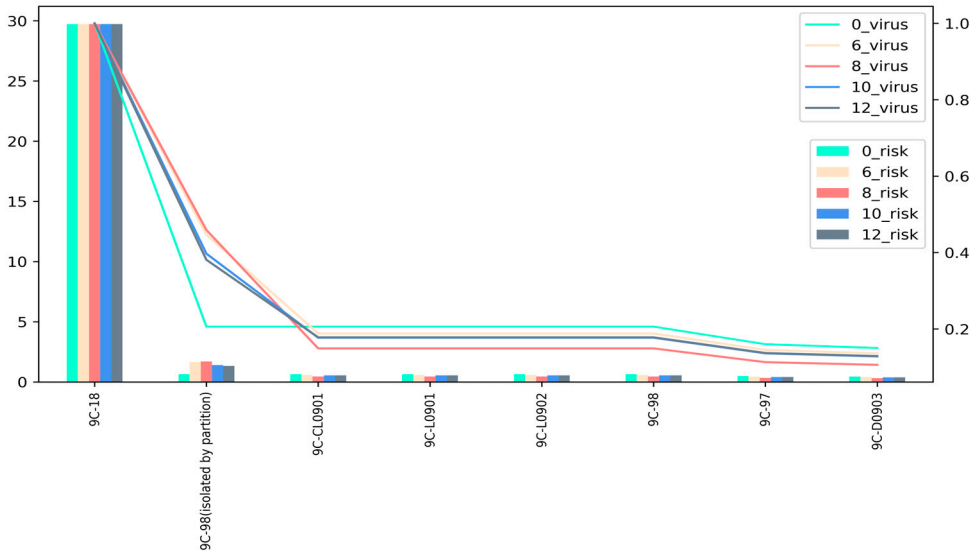

Figure 7. Changes in the virus concentration and infection probability in each room under five scenarios (VC_x means virus concentration after adding one partition every x room; IP means infection probability).

Table 8 displays the estimated number of virus spread zones (excluding the corridor) and the total number of infected individuals under the five scenarios.

Table 8. Estimated number of virus dissemination zones (excluding the corridor) and total number of infected individuals under the five scenarios.

	No Increase in Partitions	Add One Partition Every 12 Rooms	Add One Partition Every 10 Rooms	Add One Partition Every 8 Rooms	Add One Partition Every 6 Rooms
Number of virus spread areas	6	6	6	6	6
Estimated number of infected individuals	2.41	2.35	2.35	2.29	2.37

The chart above illustrates a reduction in the overall infection risk for the entire ship as the number of partitions within the corridor area increases incrementally (the number of partitions increases from left to right in Table 8). The estimated number of infected individuals was reduced from 2.41 to 2.29. This is because adding partitions will increase the virus concentration within the isolated corridor segment, consequently diminishing the virus concentration in the remaining areas. In this case, the optimal partition density setting would be one partition per eight rooms. However, overall, the addition of partitions has a limited impact on reducing the risk of virus infection.

3.3.2. Adding Filters to the System

To reduce the number of infected individuals in different scenarios, high-efficiency filters can be placed in public areas. The stable concentration of indoor contaminants after filtering in this study was calculated as the stable concentration of the multi-zone airflow simulation after adding the filter air volume to dilute. The calculation method is as follows:

$$c_t = \frac{c_o V}{V + \eta Q}$$

where c_t is the final stable concentration of indoor contaminant after using the filter, c_o is the stable concentration of indoor contaminant extracted from multi-zone airflow simulations, V is the volume of the zone, Q is the purified air volume of the filter per hour, and η is the filter efficiency.

A sub-HEPA filter with a filtration efficiency of 99% was placed in the public area where the patient is located, and the estimated total number of infected individuals with an hour of exposure before and after placing the filter was calculated. In addition, the purification air volume per hour of filtration was set to 0.5, 1, 2, and 4 times the current zone's air supply volume to study the optimal one-hour purification air volume to reduce the risk of infection. For the case without the filter, the calculation of the estimated total number of infections was the same as that in Section 3.1.2. For the case with the use of filters, according to the rules of many simulation results, the number of infections is concentrated in the source area. Therefore, the specific calculation steps are as follows:

(1) Carry out a multi-zone airflow simulation and output a stable concentration of virus in each region;
(2) Calculate the final stable concentration in the area where the filter is used according to Function (4);
(3) Calculate the ratio p of the virus concentration in the region where the patient stays before and after filtering and multiply it by the simulated virus concentration in each area to estimate the virus concentration in other regions (outside the region where the patient stays) after using the filter;
(4) Use Function (3) to calculate the total number of infected individuals in the entire ship after using the filter.

Figure 8 shows the estimated number of infected individuals with and without the use of filters at different purification airflow rates. The results show that the total number of infected people was reduced by more than 75% after using the filter. This is because the virus concentration in the source side was greatly reduced after filtering. Filtration has the greatest effect on reducing the risk of infection when the purification air volume of the filter is half the supply air volume. If the purification air volume is increased, then the energy consumption increases, but little improvement in infection control is observed. Hence, it is advisable to place a filter in public areas during an epidemic to mitigate the risk of infection. The recommended air purification volume per hour for the filter should be set at half of the air supply volume within the designated space.

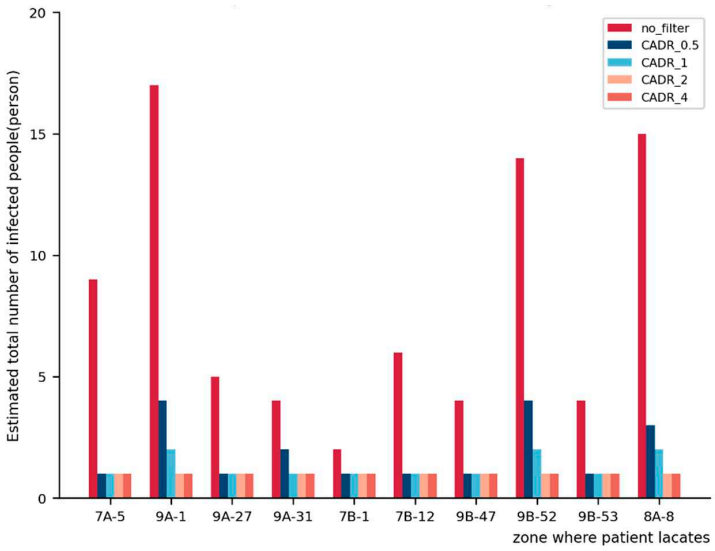

Figure 8. Changes in the number of infected individuals before and after adding filters to the system (CADR_x means the purification air volume per hour of filtration was x times the current zone's air supply volume).

4. Conclusions

This study established a multi-zone infection quantitative risk assessment model of airborne virus transmission to research virus transmission mechanisms and countermeasures in large ships during an epidemic. This innovative approach combines a multi-zone airflow model with the Wells–Riley model, marking its pioneering application in the domain of large-scale cruise ships. The results of the case study indicate that the number of isolated rooms shall be at least 5% of the total occupancy. Two strategies were evaluated. Firstly, adding partitions to long corridors appears to have a somewhat lesser impact compared to the inclusion of air filters in mitigating the spread of the virus. Secondly, the placement of sub-HEPA filters in areas where patients are located has the potential to reduce the probability of infection by more than 75%. Considering energy consumption and the effect of risk reduction, the purification air volume per hour should be set at half of the room supply air volume according to our research. The proposed method can not only facilitate the quantification of infection risks within multi-zone indoor environments but also aid in determining optimal isolation locations, estimating the requisite number of isolation rooms during the initial round of epidemic transmission, and furnishing valuable guidance for the implementation of effective epidemic prevention measures.

5. Limitation and Future Work

This study has several limitations. In the case study, we endeavored to simulate the spread of SARS-CoV-2 on the target cruise ship by using parameters derived from measles. With the constant variation of Omicron, measles may not be suitable. Any extrapolation of our findings to the most recent Omicron variant should be approached cautiously. Secondly, this study does not address specific strategies for HVAC (heating, ventilation, and air-conditioning) system design. Future research should encompass this crucial aspect. Thirdly, our research is focused on the whole ship, regarding each area as a well-mixed space and unable to show the virus distribution inside the zones. Subsequent investigations will consider the intricacies of virus distribution within large spaces, taking inter-zonal airborne transmission into account. Moreover, the outcomes derived from the airflow model simulations presented in this article warrant empirical validation. Furthermore, there is potential for future research to utilize Particle Image Velocimetry to visualize contaminant dispersion within these zones. The infection probability calculated based on the Wells–Riley model needs to be verified with real infection data. Regrettably, the requisite empirical data for such validations are currently unavailable, thereby imposing limitations on our ability to corroborate the results.

Author Contributions: Methodology, Z.X., H.G. and P.X.; Software, Z.X. and H.G.; Formal analysis, Z.X., H.G., Z.Q. and P.X.; Writing—original draft, Z.X.; Writing—review & editing, Z.X., H.G., Z.Q. and P.X.; Supervision, P.X. and Z.Q. All authors have read and agreed to the published version of the manuscript.

Funding: This research was funded by China Southern Power Grid, grant number GDKJXM 20200569.

Data Availability Statement: Data is unavailable due to commercial restrictions.

Conflicts of Interest: The authors declare no conflict of interest.

Appendix A

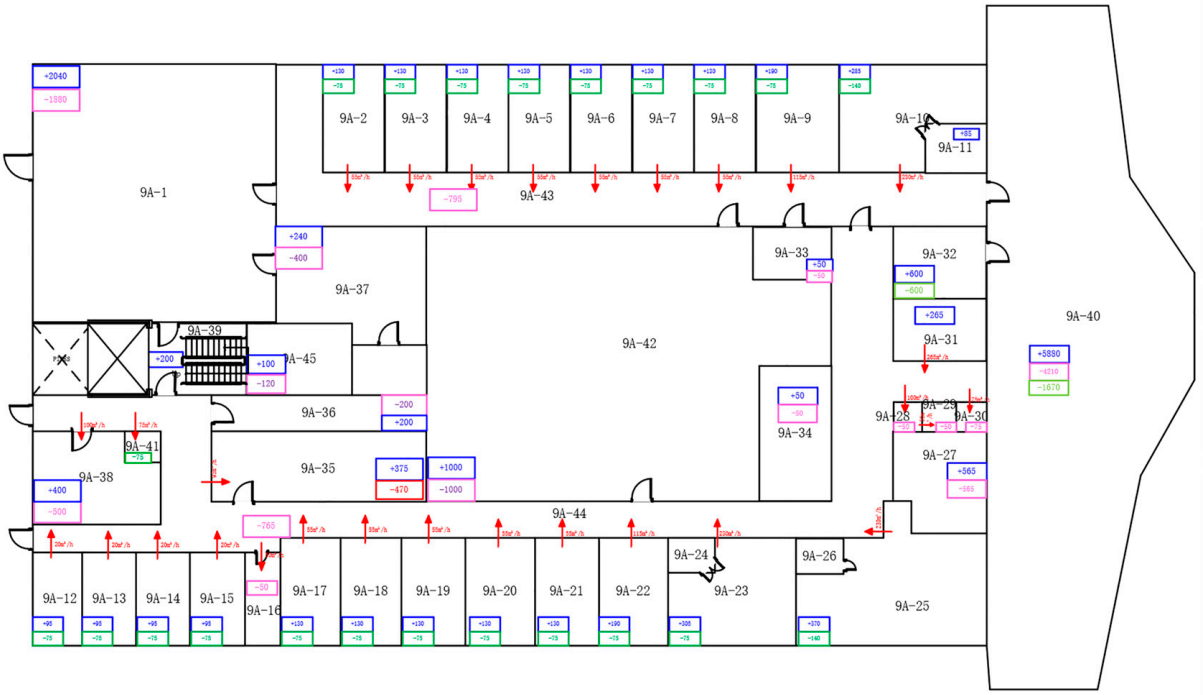

(**a**) Ninth floor A area.

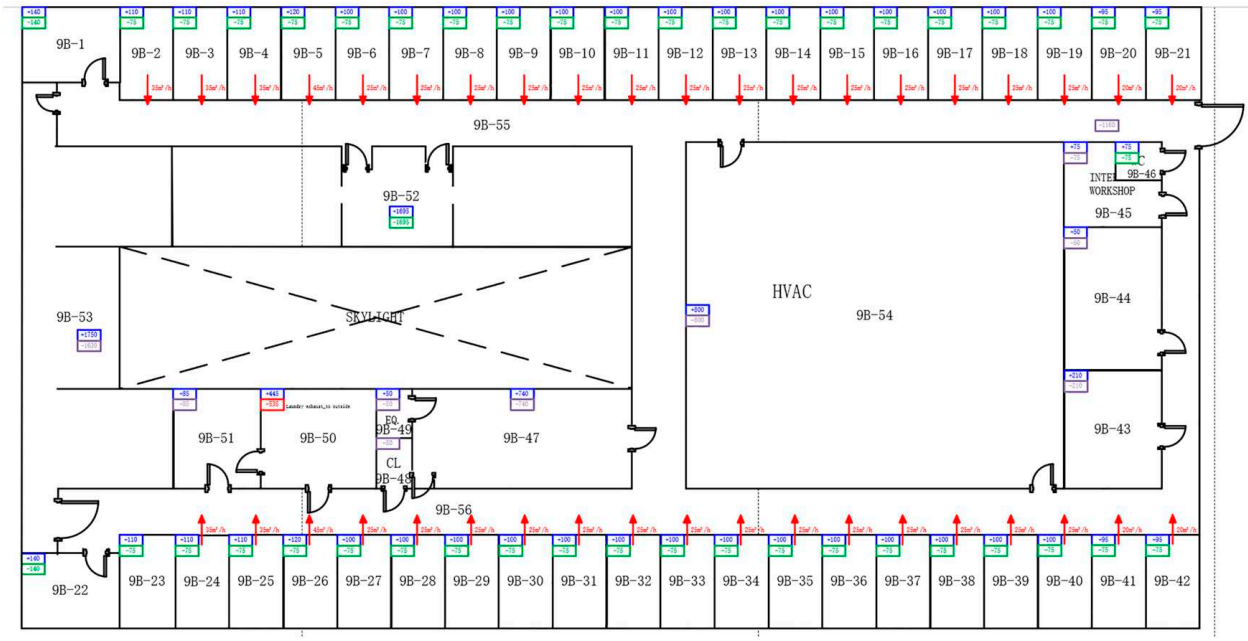

(**b**) Ninth floor B area.

Figure A1. *Cont.*

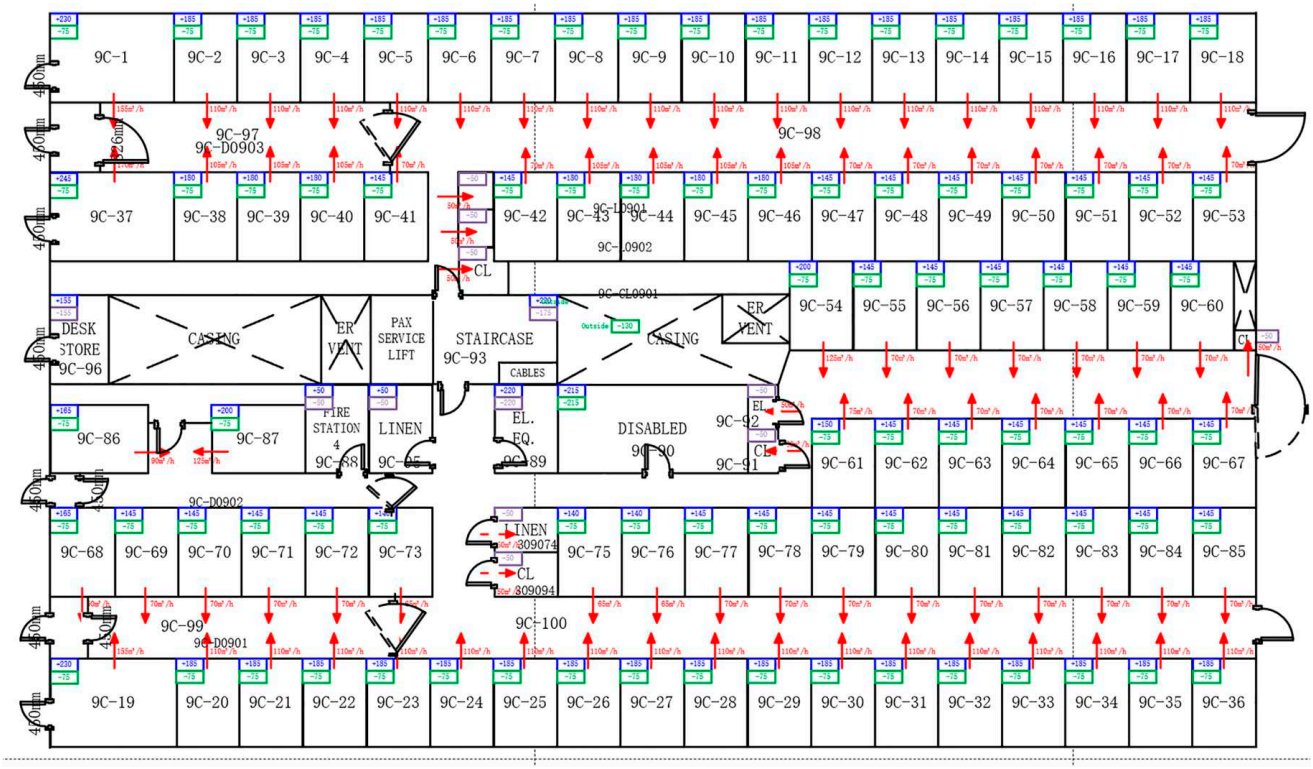

(**c**) Ninth floor C area.

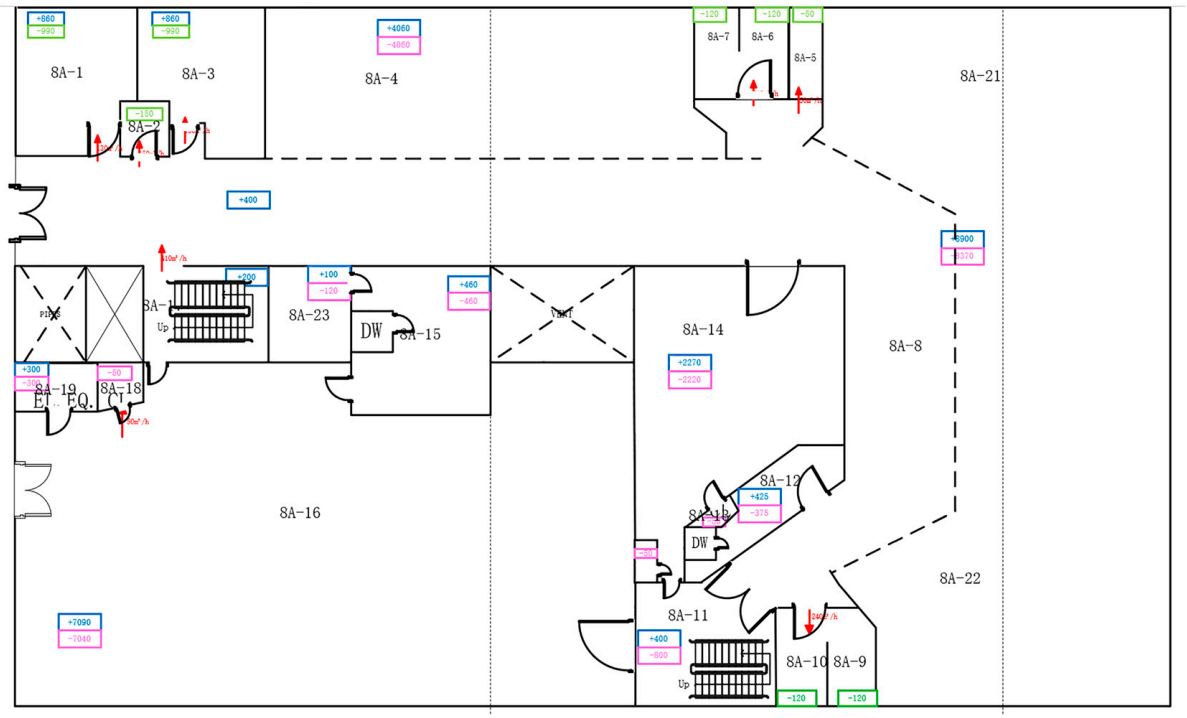

(**d**) Eighth floor A area.

Figure A1. *Cont.*

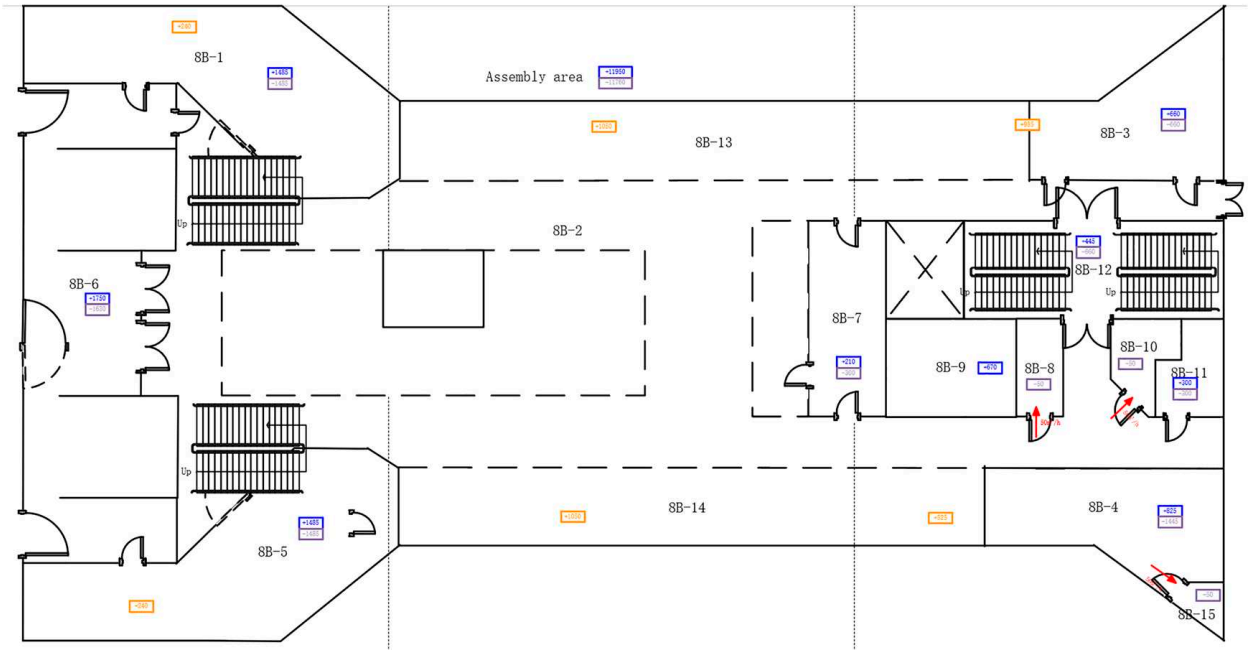

(**e**) Eighth floor B area.

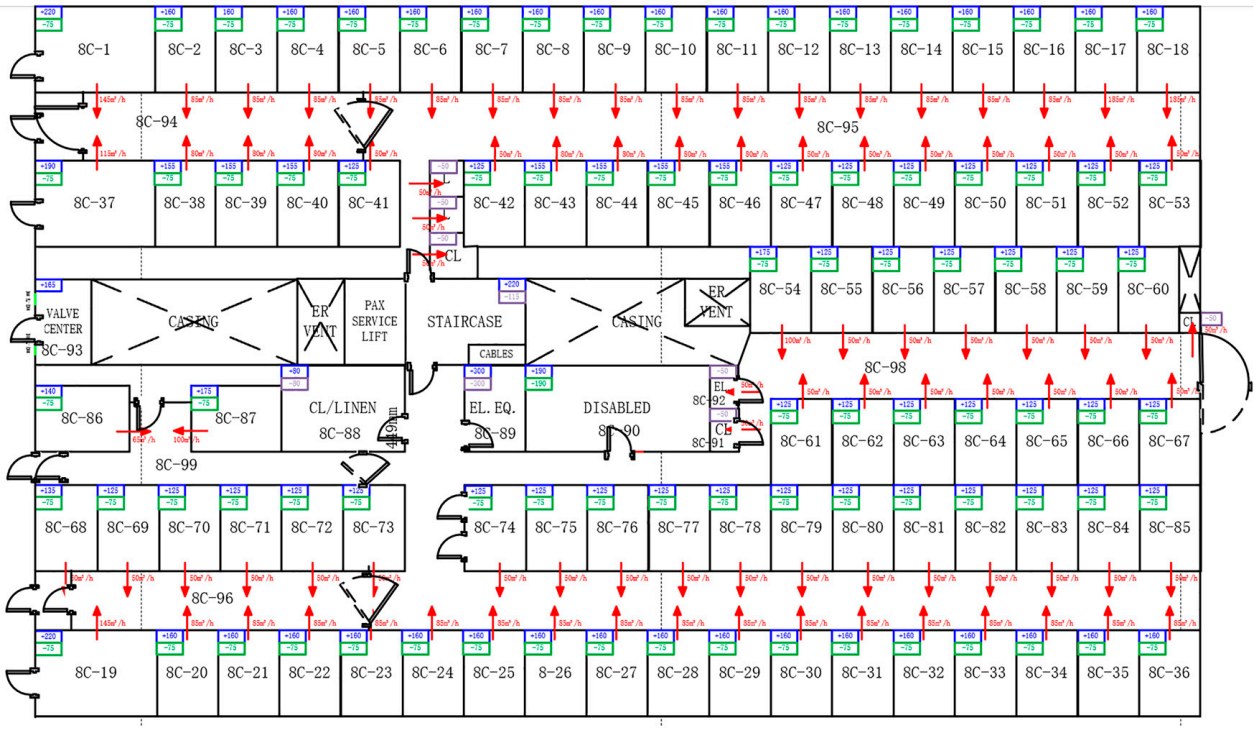

(**f**) Eighth floor C area.

Figure A1. *Cont.*

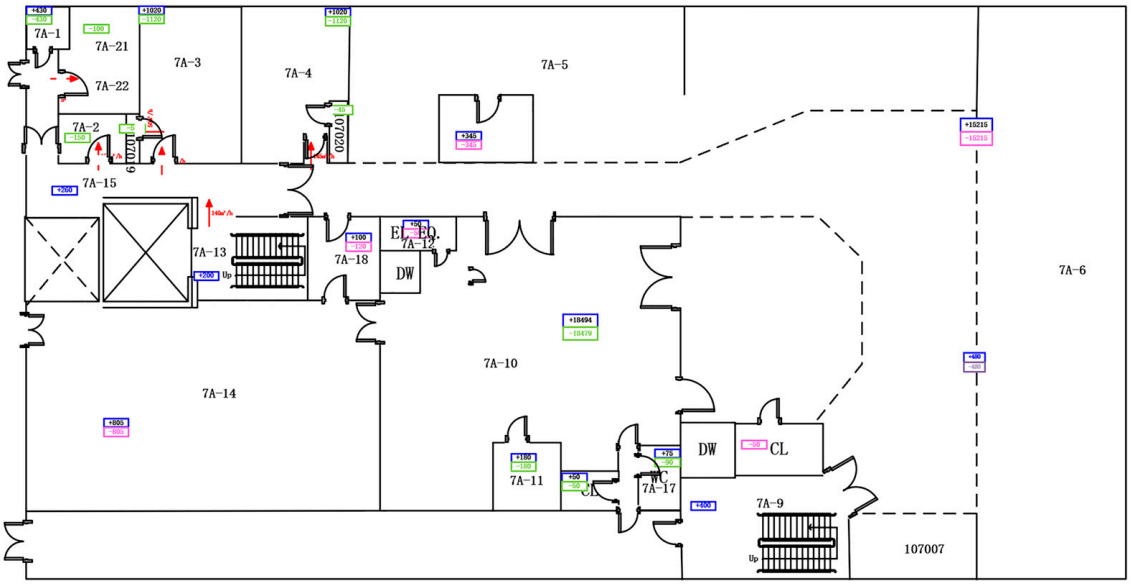

(**g**) Seventh floor A area.

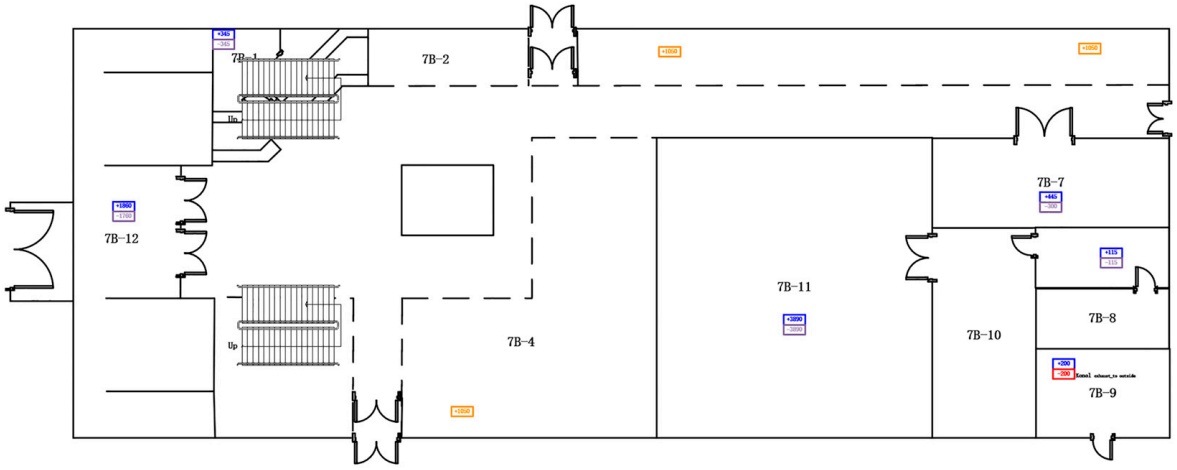

(**h**) Seventh floor B area.

Figure A1. Layout of the ship in the case study (only personnel activity area is shown).

References

1. Zhang, J.; Wu, B.; Yan, X. A Method for Risk Assessment of COVID-19 Infection on Large Cruise Ships. *J. Transp. Inf. Saf.* **2020**, *38*, 112–119. [CrossRef]
2. Ito, H.; Hanaoka, S.; Kawasaki, T. The cruise industry and the COVID-19 outbreak. *Transp. Res. Interdiscip. Perspect.* **2020**, *5*, 100136. [CrossRef] [PubMed]
3. Guo, M.; Xu, P.; Xiao, T.; He, R.; Dai, M.; Miller, S.L. Review and comparison of HVAC operation guidelines in different countries during the COVID-19 pandemic. *Build. Environ.* **2021**, *187*, 107368. [CrossRef] [PubMed]
4. Wang, Z.; Galea, E.R.; Grandison, A.; Ewer, J.; Jia, F. A coupled Computational Fluid Dynamics and Wells-Riley model to predict COVID-19 infection probability for passengers on long-distance trains. *Saf. Sci.* **2022**, *147*, 105572. [CrossRef] [PubMed]
5. Riley, R.L.; Riley, E.C.; Murphy, G. Airborne Spread of Measles in a Suburban Elementary-School. *Am. Rev. Respir. Dis.* **1978**, *107*, 421–432. [CrossRef] [PubMed]
6. Sun, C.; Zhai, Z. The efficacy of social distance and ventilation effectiveness in preventing COVID-19 transmission. *Sustain. Cities Soc.* **2020**, *62*, 102390. [CrossRef]
7. Aganovic, A.; Bi, Y.; Cao, G.; Kurnitski, J.; Wargocki, P. Modeling the impact of indoor relative humidity on the infection risk of five respiratory airborne viruses. *Sci. Rep.* **2022**, *12*, 11481. [CrossRef]
8. Rudnick, S.N.; Milton, D.K. Risk of indoor airborne infection transmission estimated from carbon dioxide concentration. *Indoor Air* **2003**, *13*, 237–245. [CrossRef]

9. Zhang, S.; Lin, Z. Dilution-based evaluation of airborne infection risk-Thorough expansion of Wells-Riley model. *Build. Environ.* **2021**, *194*, 107674. [CrossRef]
10. Ko, G.; Thompson, K.M.; Nardell, E.A. Estimation of tuberculosis risk on a commercial airliner. *Risk Anal.* **2004**, *24*, 379–388. [CrossRef] [PubMed]
11. Aganovic, A.; Bi, Y.; Cao, G.; Drangsholt, F.; Kurnitski, J.; Wargocki, P. Estimating the impact of indoor relative humidity on SARS-CoV-2 airborne transmission risk using a new modification of the Wells-Riley model. *Build. Environ.* **2021**, *205*, 14. [CrossRef] [PubMed]
12. Vuorinen, V.; Aarnio, M.; Alava, M.; Alopaeus, V.; Atanasova, N.; Auvinen, M.; Balasubramanian, N.; Bordbar, H.; Erästö, P.; Grande, R.; et al. Modelling aerosol transport and virus exposure with numerical simulations in relation to SARS-CoV-2 transmission by inhalation indoors. *Saf. Sci.* **2020**, *130*, 104866. [CrossRef] [PubMed]
13. Borro, L.; Mazzei, L.; Raponi, M.; Piscitelli, P.; Miani, A.; Secinaro, A. The role of air conditioning in the diffusion of SARS-CoV-2 in indoor environments: A first computational fluid dynamic model, based on investigations performed at the Vatican State Children's hospital. *Environ. Res.* **2021**, *193*, 110343. [CrossRef] [PubMed]
14. Yamakawa, M.; Kitagawa, A.; Ogura, K.; Chung, Y.M.; Kim, M. Computational investigation of prolonged airborne dispersion of novel coronavirus-laden droplets. *J. Aerosol Sci.* **2021**, *155*, 15. [CrossRef] [PubMed]
15. Qian, H.; Li, Y.; Nielsen, P.V.; Huang, X. Spatial distribution of infection risk of SARS transmission in a hospital ward. *Build. Environ.* **2009**, *44*, 1651–1658. [CrossRef]
16. Yan, Y.; Li, X.; Shang, Y.; Tu, J. Evaluation of airborne disease infection risks in an airliner cabin using the Lagrangian-based Wells-Riley approach. *Build. Environ.* **2017**, *121*, 79–92. [CrossRef]
17. Foster, A.; Kinzel, M. Estimating COVID-19 exposure in a classroom setting: A comparison between mathematical and numerical models. *Phys. Fluids* **2021**, *33*, 021904. [CrossRef]
18. Pang, S.; Xiao, J.; Fang, Y. Risk assessment model and application of COVID-19 virus transmission in closed environments at sea. *Sustain. Cities Soc.* **2021**, *74*, 103245. [CrossRef]
19. Chen, Q. Ventilation performance prediction for buildings: A method overview and recent applications. *Build. Environ.* **2009**, *44*, 848–858. [CrossRef]
20. Tian, W.; Han, X.; Zuo, W.; Sohn, M.D. Building energy simulation coupled with CFD for indoor environment: A critical review and recent applications. *Energy Build.* **2018**, *165*, 184–199. [CrossRef]
21. Wang, K.; Zhang, Q.; Zhang, G.Q.; Shi, Y.L.; Deng, T.F. Airflow and indoor air quality of residence heating by charcoal basin in rural region. *J. Cent. South Univ. Technol.* **2007**, *14*, 81–85.
22. Cheng, P.; Chen, W.; Xiao, S.; Xue, F.; Wang, Q.; Chan, P.W.; You, R.; Lin, Z.; Niu, J.; Li, Y. Probable cross-corridor transmission of SARS-CoV-2 due to cross airflows and its control. *Build. Environ.* **2022**, *218*, 14. [CrossRef] [PubMed]
23. Szczepanik-Scislo, N. Improving Household Safety via a Dynamic Air Terminal Device in Order to Decrease Carbon Monoxide Migration from a Gas Furnace. *Int. J. Environ. Res. Public Health* **2022**, *19*, 1676. [CrossRef] [PubMed]
24. Heibati, S.; Maref, W.; Saber, H.H. Assessing the Energy, Indoor Air Quality, and Moisture Performance for a Three-Story Building Using an Integrated Model, Part Two: Integrating the Indoor Air Quality, Moisture, and Thermal Comfort. *Energies* **2021**, *14*, 5648. [CrossRef]
25. Pease, L.F.; Wang, N.; Salsbury, T.I.; Underhill, R.M.; Flaherty, J.E.; Vlachokostas, A.; Kulkarni, G.; James, D.P. Investigation of potential aerosol transmission and infectivity of SARS-CoV-2 through central ventilation systems. *Build. Environ.* **2021**, *197*, 107633. [CrossRef]
26. Yan, S.; Wang, L.; Birnkrant, M.J.; Zhai, Z.; Miller, S.L. Multizone Modeling of Airborne SARS-CoV-2 Quanta Transmission and Infection Mitigation Strategies in Office, Hotel, Retail, and School Buildings. *Buildings* **2023**, *13*, 102. [CrossRef]
27. Dols, W.S.; Polidoro, B. *CONTAM User Guide and Program Documentation Version 3.4*; National Institute of Standards and Technology: Gaithersburg, MD, USA, 2020; p. 1. [CrossRef]
28. Andrews, L. Omicron Sub Variant BA.2 just as Contagious as MEASLES, Says Former World Health Organization Official, in DailyMail. UK. 2022. Available online: https://www.dailymail.co.uk/news/article-10614413/Omicron-sub-variant-BA-2-just-contagious-MEASLES.html (accessed on 15 March 2022).
29. Guerra, F.M.; Bolotin, S.; Lim, G.; Heffernan, J.; Deeks, S.L.; Li, Y.; Crowcroft, N.S. The basic reproduction number (R-0) of measles: A systematic review. *Lancet Infect. Dis.* **2017**, *17*, e420–e428. [CrossRef]